Available online at www.sciencedirect.com
ScienceDirect
Cement and Concrete Research 37 (2007) 1085–1095
Cement and Concrete Research

Degradation of concrete by flue gases from coal combustion

Vladimír Pavlík *, Adolf Bajza, Ildikó Rouseková, Stanislav Unčík, Marián Dubík

Department of Material Engineering, Faculty of Civil Engineering, Slovak University of Technology, Radlinského 11, 813 68 Bratislava, Slovak Republic

Received 2 June 2006; accepted 16 April 2007

Abstract

The effect of flue gases from coal combustion on the concrete shell of a power plant stack was analyzed and the damage to the concrete was evaluated. The compressive and tensile strengths of concrete were determined by rebound hammer test and pull-off test on the site. Samples of concrete taken from various zones of the stack shell were analyzed in detail. The examination techniques used included chemical analysis, water suspension analyses, XRD, thermal analysis, SEM and EDS. It was found that the flue gases and the acid condensate, acted very aggressively at an elevated temperature and caused severe degradation of the inside surface zone of the concrete shell. The binding material in this zone was converted into sulfur-bearing compounds. Gypsum was identified as the dominant compound in the degraded zone of concrete in the upper parts, while anhydrite in the lower parts of the stack. Carbonated zone was located below the clearly delimitated sulfated zone of the concrete. The aggressive environment in the stack did not affect the internal zones in the concrete.

Keywords: Carbonation; Degradation; Concrete; Portland cement; Sulfur dioxide

1. Introduction

Combustion of coal produces flue gases with various content of acidic components that act aggressively on the concrete. Flue gas stacks of coal-fired power plants are therefore commonly composed of an outer shell from reinforced concrete and an internal lining system that protects the inner surface of concrete shell from high temperatures and chemical attack. An attack by the flue gases usually occurs when the internal protective lining in the stack is imperfectly made or damaged. The type and concenration of the acidic components in the flue gases, concentration of oxygen, elevated temperature, fluctuation of humidity and eventual moisture condensation affects degradation processes in concrete. Chemical reactions causing corrosion of concrete mainly include those of carbon dioxide, sulfur dioxide and trioxide, nitrogen oxides and aerosol/vapor mixture or condensate of sulfuric primarily with products of cement hydration. Carbon dioxide converts calcium hydroxide and eventually also hydrated calcium silicates and aluminates into calcium carbonate. Sulfur oxides and sulfuric acid can react with all the calcium compounds of hydrated cement, including calcium carbonate, and convert them into sulfur-bearing compounds. These compounds usually form sulfate/sulfite deposits on an internal side of the concrete surface of the stack. The list of sulfur-bearing compounds that mainly come under consideration includes calcium sulfite ($CaSO_3 \cdot 1/2H_2O$), calcium sulfates ($CaSO_4$, $CaSO_4 \cdot 1/2H_2O$ and $CaSO_4 \cdot 2H_2O$) and calcium sulfoaluminates ($3CaO \cdot Al_2O_3.CaSO_4 \cdot 12H_2O$ and $3CaO \cdot Al_2O_3.3CaSO_4 \cdot 31–32H_2O$). Each compound may be formed and exists only under defined conditions.

Calcium sulfoaluminates can hardly be expected in the carbonated and sulfated surface zones of concrete, as both carbonation and sulfation reduce the pH value of concrete below their zone of stability. Damidot and Glasser [1] reported that ettringite is stable at 25 °C at pH values ranging from 10.43 to 12.52. According to other authors [2,3] the boundary for the disappearance of ettringite at 20 °C was at $pH \leq 10.7$ and for monosulfoaluminate at $pH \leq 11.6$ [2]. At 50 °C ettringite is stable at pH values ranging from 10.52 to 12.41, and at 85 °C at pH values from 10.87 to 12.25 [1].

* Corresponding author. Tel.: +421 7 59274691; fax: +421 7 52494357.
E-mail address: vladimir.pavlik@stuba.sk (V. Pavlík).

0008-8846/$ - see front matter © 2007 Elsevier Ltd. All rights reserved.
doi:10.1016/j.cemconres.2007.04.008

In contrast to the calcium monosulfoaluminate, the ettringite in hardened cement paste is a stable phase in the presence of calcium carbonate. However, the stability of ettringite is probably reduced in a strongly carbonated concrete with a substantially lowered pH value. Ettringite's decomposition due to carbonation was reported by authors [4–8]. Reaction products under wet conditions were calcium carbonate, gypsum and alumina gel. Ettringite also quickly dissolves in acid solutions. Shi and Stegemann [5] expressed the reaction as follows:

$$C_3A.3CaSO_432H_2O + 12H^+ = 3Ca^{2+} + 2Al^{3+} + 3[CaSO_42H_2O] + 32H_2O \quad (1)$$

There are numerous references regarding the sulfation of concrete, lime or limestone in gaseous environment under various conditions. Research findings on deterioration of historical monuments by a polluted urban atmosphere are also relevant here [9].

An investigation of carbonation and sulfation of cellular concrete and other of cement-based materials exposed to an artificial atmosphere with a high concentration of CO_2 and SO_2 revealed that both processes take place simultaneously [10–13]. Sulfation takes place only near the surface and does not have a retarding effect with regard to further carbonation in the deeper-lying zones of the concrete. The reaction products were mostly $CaSO_3 \cdot 1/2H_2O$, $CaSO_4 \cdot 1/2H_2O$ and $CaSO_4 \cdot 2H_2O$. While gypsum was usually identified in the humid atmosphere, sulfite prevailed at a lower humidity [13]. Carbonation products were among the first to be attacked by SO_2 and humidity was the dominant factor in controlling the rate of decomposition of $CaCO_3$ at a lower concentration of SO_2.

The investigation of processes of flue gas desulfurization (FGD) also brought out some relevant findings [14–18]. In the FGD processes, the solid sorbent, usually $Ca(OH)_2$ or $CaCO_3$ of high fineness, is brought into contact with flue gases at elevated temperatures in order to scrub the SO_2 gas from them. The amount of time the flue gas and solid phases lasts in the reactors is in terms of seconds. Generally, the FGD residue is composed of sulfate, sulfite or a mixture of both. The rate of reaction between various phases is strongly affected by humidity and the concentration of SO_2. The humidity is of particular importance especially in the case of a reaction between $CaCO_3$ and SO_2. The reaction rate of $CaCO_3$ with SO_2 was reported to be virtually zero at a relative humidity below 20%; however, above this point it increased exponentially [19]. When hydrated lime was used as a sorbent, carbonation and sulfating reactions with $Ca(OH)_2$ occurred simultaneously [14–18]. The reaction product was $CaSO_3 \cdot 1/2H_2O$, which further reacted with oxygen in the humidified flue gas to form gypsum.

Condensation of moisture from the flue gas can dramatically enhance the aggressiveness of the environment in the stack. Condensation occurs when flue gases cool down below the dew point temperature. Condensate with the lowest aggressiveness occurs when the flue gases contain only CO_2 and water. The dew point temperature of such a condensate is usually about 55–60 °C and the condensate is neutral or only slightly acidic. However, flue gases from coal combustion always contain sulfur oxides and also other acidic compounds. The condensate therefore usually represents a solution of various acids, where sulfuric acid prevails. Most of the sulfur in the flue gases is in the form of sulfur dioxide and usually much less than 5% is in the form of sulfur trioxide [20–23]. When the flue gas temperature drops, the sulfur trioxide combines with water to form sulfuric acid vapors. If the gases cool further, the sulfuric acid starts to condense. Sulfuric acid condense as the first, even when there are other types of acids present in the exhaust gases, such as sulfurous, nitric, hydrochloric and hydrofluoric acids — due to its highest dew point temperature of all of them [24]. Therefore, the term "acid dew point", which is usually defined in connection with combustion processes, corresponds to the dew point of sulfuric acid. Even a very low concentration of SO_3 in exhaust gases causes a substantial increase in the dew point temperature and produces a condensate with a high concentration of sulfuric acid. It is caused by an extreme difference between the boiling points of water (100 °C) and pure sulfuric acid (338 °C) [22]. The concentration of sulfuric acid in the condensate depends mostly on the humidity, concentration of SO_3 (SO_2) and the temperature of the flue gases [21,22,24]. Concentration of sulfuric acid in the condensate lying in a range from 65 to 95% and a dew point temperature ranging from about 100 °C to 150 °C or even up to 180 °C was reported by some authors [21,22,24]. When temperature decreases below the dew point of water, the condensing water will dilute the acid solution.

The effect of NO_x on calcareous materials is less documented. However, study of Martínez–Ramírez et al. [25] has proved that SO_2 atmospheres are more aggressive for lime mortars than NO_x environments.

2. Object of study and technological conditions

The 150 m high concrete stack of a power plant station was scheduled for repair. Prior to the repair works the actual condition of the concrete shell of the stack had to be determined.

The concrete shell of the stack was protected from inside by a lining composed of acid-resistant fire-clay blocks with one enameled side. Bricks from fired diatomite provided the heat insulation of the concrete. The concrete was made from Portland cement corresponding to CEM I 42.5. Later the polymer-composite material containing an embedded glass fiber-reinforcing mattress was used for protection of the stack. After 1 year of service, the protective material was damaged in a large area.

The stack has been in operation about 36 years. After the first 34 years, a desulfurization technology system composed of two desulfurization units was installed. Since that time the composition and temperature of the flue gases has varied depending on the regime of the desulfurization process in operation. When the desulfurization process is in operation, the temperature of the flue gases decreases and the humidity increases (Table 1). The temperature of the flue gases is measured behind electrofilters, prior to their entry into the stack. After about one year since the desulfurization units were

Table 1
Chemical composition and temperature of flue gases; theoretical values of acid dew point temperatures were calculated for two different percentages of SO_2 to SO_3 conversion

Chemical composition (%)	Technological conditions — number of desulfurization units in operation		
	Without desulfurization	One unit in operation (combined regime)	Two units in operation (desulfurization regime)
N_2	67.27	66.00	64.50
O_2	5.11	5.25	5.40
H_2O	15.94	17.95	19.97
CO_2	11.32	11.00	10.28
SO_x [a]	0.33	0.17	0.02
$NO_\times$	0.03	–	–
Average temperature	175 °C	135 °C	90 °C
Acid dew point temperature	161 °C (2%) 171 °C (5%)	155 °C (2%) 165 °C (5%)	136 °C (2%) 145 °C (5%)

[a] Concentration of SO_x in the flue gases was taken as SO_2 concentration.

installed the stack was finally put out of action and inspected for damage. In the one-year long period different desulfurization regimes had been in operation and also some short interruptions of the desulfurization process took place.

To estimate the occurrence of the acid condensation in the stack, we calculated the approximate values of the acid dew point temperatures from the composition of the flue gases (Table 1). The acid dew point temperatures were calculated using Eq. (2) given by Verhoff and Banchero [23].

$$1000/T_{DP} = 2.276 - 0.0294\ \ln(P_{H2O}) - 0.0858\ \ln(P_{H2SO4}) + 0.0062\ \ln(P_{H2O})\ .\ln(P_{H2SO4}) \quad (2)$$

where:

T_{DP} Dew point temperature of H_2SO_4 (K);
P_{H2O} partial pressure of the flue gas moisture (mm Hg);
P_{H2SO4} partial pressure of the H_2SO_4 (mm Hg) that is equal or near to P_{SO3} at temperatures below 200 °C [21]. 2% and 5% conversion of SO_2 to SO_3 was assumed.

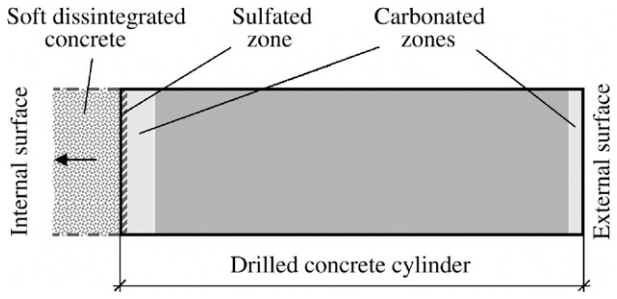

Fig. 1. Schematic view of the concrete zones arranged normal across the stack wall. Depiction of carbonated and sulfated zones location is based on results of analyses described further.

Table 2
Samples of degraded concrete from the internal side of the stack shell

Sample designation	Height above the ground (m)
K-01-1	123
K-01-2	123
K-01-3	107
K-01-4	80
K-01-5	71
K-01-6	54
K-01-7	34
K-01-8	17

The data in Table 1 show that the average temperature of the undesulfurized flue gas behind electrofilters is slightly higher than the calculated acid dew point temperature of this gas. In this case the sulfuric acid is supposed to condense later in the flue gas stream, after the gas is cooled beneath the acid dew point temperature in the stack, or on cooler surfaces in a space between the liner and the stack shell. However, the average temperatures of the desulfurized flue gases are lower than their calculated acid dew point temperatures. In this case an acid aerosol/vapor mixture of sulfuric acid is supposedly present in the flue gas stream already at the inlet into the stack. These facts indicate that the inner surface of the concrete shell could come into contact also with sulfuric acid aerosol or condensate, regardless of what technological regime was in operation.

3. Experimental

3.1. Inspection of concrete shell

The concrete shell was visually inspected at various heights above the ground. The inspection revealed a surface zone of totally degraded concrete along the entire inside periphery of the stack shell and throughout the height of the stack (Fig. 1). Soft crumbling zone of degraded concrete in the uppermost part of the stack shell (in heights from 123 to150 m) was mostly about 30 mm thick. In lower parts of the stack (in heights from 34 to 85 m) the surface zone of degraded concrete was about 10 mm thick. Section 3.2.1 of this paper describes the visual character of the degraded concrete, while the results of the analysis of degraded concrete are presented in Section 4.1. The concrete underneath the degraded zone was compact with no steel rebar protruding from it. A small number of vertical cracks about 2 to10 mm wide were observed in the sound concrete after the degraded surface zone was removed by sandblasting.

3.2. Research scheme

Research work was aimed at evaluating the degradation effect of flue gases on concrete. Research scheme consisted of three phases as follows:

a) analysis of the degraded concrete from the internal surface of the stack shell;
b) analysis of the concrete core that was drilled out from the stack shell;
c) determination of compressive and tensile strengths of concrete.

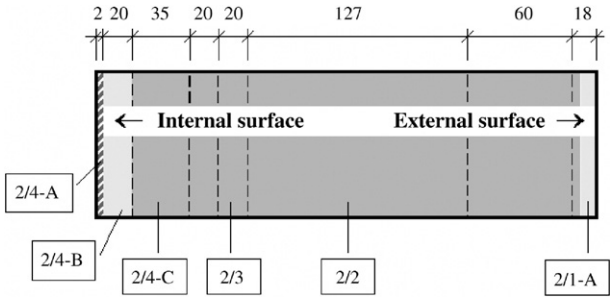

Fig. 2. Scheme of a cylindrical test specimen of concrete drilled 15 m above the ground with depiction of zones cut for chemical analysis, EDS, XRD and DTA analyses.

3.2.1. Samples of degraded concrete

Eight samples of degraded concrete from the internal surface zone were taken from eight various locations along the height of the stack shell (Fig. 1, Table 2). The obtained samples were composed of a loose white-gray mixture of dust, sand and aggregate grains of various sizes. They also contained small fragments of degraded concrete that easily crumbled into dust, sand and aggregate. Some of these fragments had yellowish color.

The obtained samples of loose bulk material were sieved through the 8 mm sieve in order to remove the large pieces of aggregate. The fraction of each sample that passed the 8 mm sieve was then carefully crushed in order to separate remaining grains of aggregate from the easily friable degraded binder. Then the sample was sieved through the 4 mm sieve. Material that passed the 4 mm sieve was again crushed and then sieved through the 2 mm sieve. Fraction passing the 2 mm sieve was then milled to fineness below 125 μm and used for analyses. The obtained sample of degraded cementitious material for analyses also contained small proportion of sand and rock particles.

Samples intended for chemical analysis and water leaching were oven-dried at 105 °C. Samples for X-ray diffraction and thermal analyses were dried only at 35 °C in order not to decompose the eventually present crystalohydrates.

3.2.2. Samples prepared from the drilled concrete core

To determine the actual state of reinforced concrete, cylindrical test specimens were drilled out from the concrete shell of the stack at various heights. The surface zone of degraded concrete was washed down from the core cylinders during drilling by water. The core that was drilled in height 15 m above the ground (Fig. 2) was subjected to wet chemical analysis, X-ray diffraction (XRD) analysis, thermal analysis (TG-DTG-DTA), observation with scanning electron microscopy (SEM) and energy dispersive X-ray spectroscopy (EDS). Conditions of testing are described in the Section 3.3.

A yellowish crust about 2 mm thick was present at the internal surface of cored concrete (Fig. 3). It is designated as 2/4-A in Figs. 2 and 3. Aggregate grains protruded from 6 to 8 mm above the surface of the crust (Fig. 3a). They were left after the surface zone of the disintegrated material was removed. The end parts of the grains were embedded in a solid concrete below. The aggregate represented siliceous river-dredged gravel or gravel from river deposits. Cementitious material beneath the yellow crust layer was gray-colored and hard, with no further observable zoning.

The concrete cylinder was cut normal into several sections, each corresponding to various depths across the stack's shell. Six of these sections were selected and sampled for analyses (Fig. 2). Concrete from each section was crushed, and the aggregate grains were then removed. The remaining fragments of cement stone, which were composed of neat hardened cement paste and a small portion of sand and fine aggregates were pulverized to a fineness below 0.09 mm and dried at 70 °C. The pulverized material was subjected to wet chemical analysis, a water suspension test, XRD and TG-DTA analyses. Surface zone of concrete was studied by using SEM and EDS.

3.2.3. Determination of the compressive and tensile strengths of concrete

Compressive strength of concrete was assessed by rebound hammer test using Schmidt test hammer, type N (Proceq SA). The measurements were made on internal side of the stack at six heights above the ground. Prior to testing the surface layer of

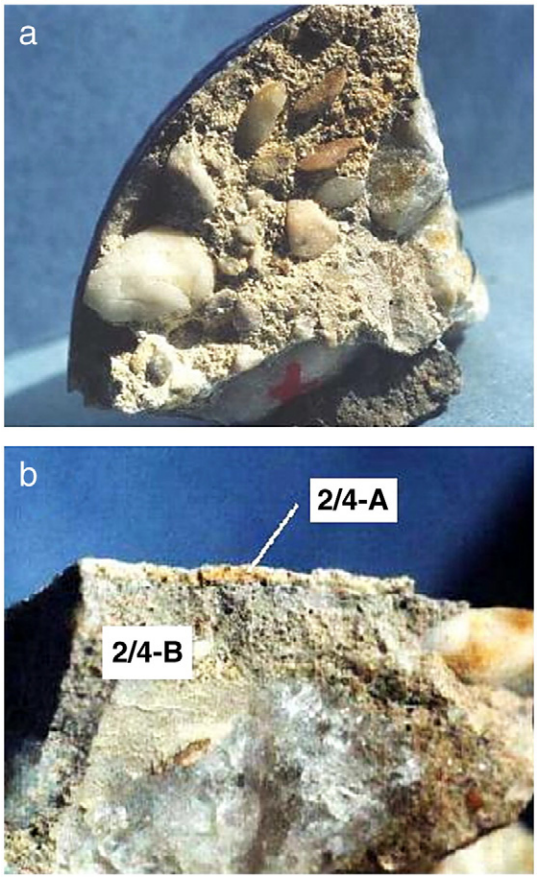

Fig. 3. Surface of the drilled cored concrete. (a) View from inside the stack. (b) Fracture normal to surface with a yellowish crust on top.

degraded concrete was removed on each test site and the concrete underneath was grind smooth.

Tensile pull-off strength of surface zones of uncorroded concrete was determined to check soundness of the substrate concrete on internal side of the stack. Dyna pull-off tester (Proceq SA) was used for the test. The test sites were also abraded prior to testing. Test sites for determination of the compressive strengths and tensile pull-off strengths were adjacent to each other.

3.3. Test methods for chemical and mineralogical analysis

3.3.1. Wet chemical analysis

The wet chemical analysis of samples of concrete was carried out in accordance with national standard STN 72 0100 [26] and European standard STN EN 196-2 [27].

3.3.2. pH of water suspensions

Water suspensions were prepared from the pulverized samples of concrete and distilled water. Samples from the degraded concrete were prepared with sample-to-water ratio 1:5 by weight; samples from the cored concrete with sample-to-water ratio 1:3. Suspensions were agitated for 10 min at a temperature of 20 °C and then the pH value of suspension was measured using pH-meter.

3.3.3. Neutralization capacity of water suspensions

Base neutralization capacities (BNC) of acid suspensions of samples of degraded concrete were determined by acid–base titration using solution of 0,1 M NaOH as a titrant and methyl orange and bromthymol blue as acid–base indicators. The amount of base (in mmol OH^-) needed to reach pH = 4.4 and pH = 7.6 for a sample of a weight of 1 g represents a base neutralization capacity to a given pH. It was abbreviated as $BNC_{4.4}$ and $BNC_{7.6}$.

3.3.4. Phenolphthalein tests

The phenolphthalein indicator test method was used to determine the zone in concrete where the alkalinity was lowered by carbonation or sulfation. Fresh fractured surfaces of the concrete were sprayed by a 3% phenolphthalein water–alcohol solution in the test. The phenolphthalein turns from uncolored to purple in a pH-range from 8.2 to 10.0.

3.3.5. Scanning electron microscopy and EDS

Energy dispersive X-ray spectroscopy (EDS) was used to determine the local elemental composition of the binding material in the drilled concrete cylinder. The fracture surfaces of concrete were imaged in a scanning electron microscope (SEM) JEOL 840A that was equipped with a KEVEX analyzer for EDS. Fracture surfaces of samples of concrete were polished to obtain precise results. Some unpolished fracture surfaces were also analyzed.

3.3.6. X-ray diffraction

The URD-6 diffractometer with a step-controlled goniometer was used for the X-ray diffraction (XRD) analysis of powdered samples. The diffractometer used CoK_α radiation and operated at 35 kV and 30 mA. Scanning from 12° to 70° 2θ by step 0.05° 2θ at a rate of 1 step/s was used.

3.3.7. Thermal analysis

Thermal analyses of the powdered samples were conducted using a G 425 Derivatograph apparatus (MOM Budapest). The operational conditions were as follows: The weight of the sample was 1 g, the sensitivity of the DTA was 1/3, the DTG 1/2, and the TG 200 mg. The sample was heated to a maximum temperature of 1200 °C at a heating rate of 10 °C/min.

4. Results

4.1. Results of analyses of degraded concrete from disintegrated surface zone

4.1.1. Chemical analysis results of degraded concrete

Results in Table 3 show that all analyzed samples from the zone of degraded concrete on internal side of the stack shell (Fig. 1) contained extremely high content of sulfates (SO_3). Molar SO_3/CaO ratio in the samples varied from 1.01 to1.21. These results indicate that all calcium bearing compounds in the cementitious material were probably decomposed and converted to calcium sulfate. However, in some samples the ratio of SO_3/CaO very significantly exceeded the value of 1.00 corresponding to formation of $CaSO_4$. We have to suppose that in these cases the sulfate ions were bound also to magnesium aluminum or iron, and/or that there could also be some free sulfuric acid (SO_3) adsorbed in the samples.

4.1.2. Water suspension's pH and BNC results

Water suspensions prepared from samples of degraded concrete were acidic to near neutral, with values for pH ranging from 2.2 to 6.8 (Table 4).

The base neutralization capacities ($BNC_{4.4}$ and $BNC_{7.6}$) of these suspensions increased with their decreasing pH values (Table 4).

Table 4 also reveals mutual relation between values for pH, basic neutralization capacity of water suspensions and SO_3/CaO ratio of samples of degraded concrete. The lowest pH and highest BNKs values were found in the suspensions that were

Table 3
Content of selected components in samples prepared from degraded concrete after partial removing of aggregate grains

Component	Chemical composition of analyzed samples (%)							
	K-01-1	K-01-2	K-01-3	K-01-4	K-01-5	K-01-6	K-01-7	K-01-8
	Height above the ground (m)							
	123	123	107	80	71	54	34	17
SiO_2+I.R.*	55.51	61.19	53.29	48.34	36.83	40.50	35.06	31.14
Aggregate left	46.38	53.03	41.50	36.35	27.62	30.82	25.80	21.57
CaO	15.62	11.32	15.25	17.95	21.81	20.23	22.65	22.68
SO_3	22.95	18.19	22.07	26.55	37.17	33.01	36.03	39.24
R_2O_3	1.22	n***	0.60	0.70	1.36	n***	1.54	1.52
LOI**	4.85	6.15	9.16	6.92	8.70	7.03	6.63	9.14
SO_3/CaO molar ratio	1.03	1.12	1.01	1.04	1.019	1.14	1.11	1.21

I.R.* — Acid insoluble residue; LOI** — Loss on ignition; n*** — Not determined.

Table 4
The pH values and base neutralization capacities (BNC) of water suspensions of degraded concrete (1:5) compared to the SO_3/CaO ratio in the samples

Sample designation	Height (m)	$BNK_{7,6}$ (0.1 mmol/g)	$BNK_{4,4}$ (0.1 mmol/g)	pH (1:5)	SO_3/CaO (molar ratio)
K-01-1	123	0.2	0	6.8	1.03
K-01-2	123	3.2	0.05	4.1	1.12
K-01-3	107	0.09	0	6.2	1.01
K-01-4	80	1.55	0.3	4.0	1.04
K-01-5	71	8.2	2.1	2.3	1.19
K-01-6	54	6.6	2.6	2.7	1.14
K-01-7	34	6.75	2.5	2.3	1.11
K-01-8	17	9.5	2.8	2.2	1.21

prepared from the samples of degraded concrete with the highest values of SO_3/CaO ratio (e.g. K-01-5,6,7,8). These findings may indicate that there is free sulfuric acid or eventually hydrolysable aluminum or iron sulfates present in the samples with the highest values of SO_3/CaO ratio.

The highest values of SO_3/CaO ratio were found in the samples of degraded concrete from heights up to 71 m in the stack (Tables 3 and 4). Water suspensions from these samples also had the highest values of BNCs and lowest values of pH. On the contrary, the samples of degraded concrete from heights above 80 m had generally lower SO_3/CaO ratio and BNKs and their water suspensions were only slightly acidic.

4.1.3. Results of XRD, thermal analyses and SEM observations of degraded concrete

Aggregate for XRD analysis was separated from the samples of degraded concrete. XRD patterns of powdered sample of aggregate of average composition showed only strong lines of quartz and very weak lines of feldspar.

Cementitious material that was separated from the degraded concrete was also analyzed by XRD (Fig. 4). Samples of degraded cementitious material from the upper parts of the stack, taken at heights of 107 m and 123 m, were composed predominantly of quartz and gypsum. Sample taken at height of 80 m contained also anhydrite with some albite, orthoclase and muscovite. On the contrary, the samples from the lower parts of the stack contained mainly anhydrite and some quartz as the dominant phases. Gypsum was identified here as a minor phase.

Table 5
Summary of DTA analysis of samples of degraded concrete taken at various stack heights

Sample	Height above the ground (m)	Main DTA endothermic effects with peaks at about			
		130–140 °C	160–170 °C	190–200 °C	760–770 °C
Compound decomposed		$SiO_2 \cdot nH_2O$	$CaSO_4 \cdot 2H_2O$	$CaSO_4 \cdot 0.5H2O$	Uncertain
K-01-2	123	Strong	Dominant	Strong	–
K-01-3	107	Weak	Dominant	Strong	–
K-01-4	80	Weak	Dominant	Strong	–
K-01-5	71	Strong	–	–	Weak
K-01-6	54	Strong	–	–	Weak
K-01-7	34	Strong	–	–	Weak
K-01-8	17	Strong	–	–	Weak

Results of thermal analyses of cementitious material from degraded concrete (Table 5 and Fig. 5) corresponded with those of XRD.

The DTA patterns of the samples from heights above 80 m shoved endothermic effects corresponding mainly to gypsum and gel of silicic acid ($SiO_2.nH_2O$). Double endothermic effects with peaks at about 160–170 °C and 190–200 °C identified gypsum; endothermic peak at about 130–140 °C corresponded to the loss of hygroscopic water from gel of $SiO_2.nH_2O$. The gel of $SiO_2.nH_2O$ was formed by decomposition of the hydrated calcium silicates in hardened cement stone by either sulfur oxides or sulfuric acid.

The DTA patterns of samples from heights from 17 m to 71 m (Fig. 5, Table 5), in contrast to previous samples, shoved a strong endothermic peak at 130–140 °C and a smaller one at 750–770 °C. The first effect at 130–140 °C corresponds to loss of hygroscopic water from the gel of $SiO_2 \cdot nH_2O$. The second at 750–770 °C is probably due to the loss of SO_3 from the aluminum sulfate or other product of cement degradation. This assumption is supported by the findings of Temuujin, et al. [28], who reported that thermal decomposition of aluminum sulfate takes place in a wide temperature range from about 570 °C to 840 °C with the peak at about 750 °C.

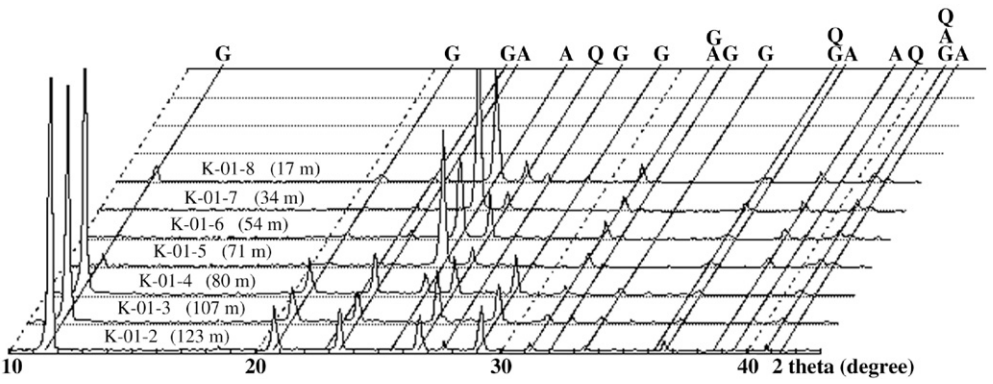

Fig. 4. XRD patterns (CuK_α radiation) of cementitious material from degraded concrete in various heights of the stack. (Phases: G — gypsum; A — anhydrite; Q — quartz).

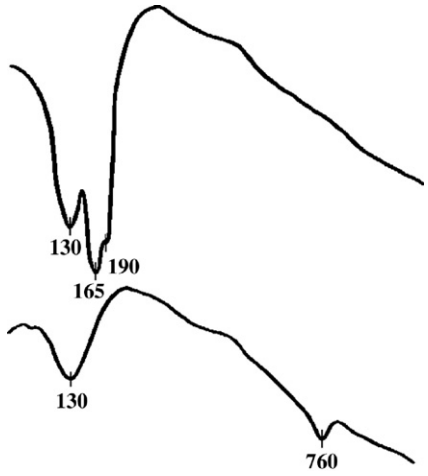

Fig. 5. Typical DTA patterns of samples of cementitious material from degraded concrete. The pattern above is for sample from height of 123 m; below for sample from 54 m.

The cause of absence of the endothermic peak at 750–770 °C in the samples from the upper parts of the stack is not quite clear. However, it can be supposed that the drop of temperature in the flue gas stream in the upper parts of the stack could cause condensation of vapors and thus lead to dissolution and leaching out of the aluminum sulfate from the degraded concrete.

Results of XRD and thermal analyses revealed that chemical and mineralogical composition of degraded concrete was strongly influenced by the temperature–humidity conditions in the stack and depended on the height in the stack. The height of about 71–80 m divided the stack into the upper and the lower regions that differed in composition of the degraded concrete. In the upper regions, at heights above 80 m there were conditions favorable for formation of gypsum, which formed by the reaction of cement binder with the SO_2, SO_3 or H_2SO_4 present in the flue gases. In the lower regions, at heights up to about 80 m in the stack, where the flue gases temperatures were higher and relative humidity values lower and where also sulfuric acid condensate with higher concentrations is to be expected — the anhydrite was formed prevailingly.

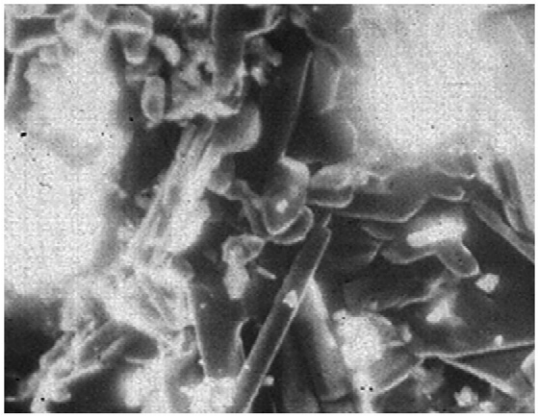

Fig. 6. SEM images of degraded concrete (3000×) from height of 123 m with crystals of gypsum.

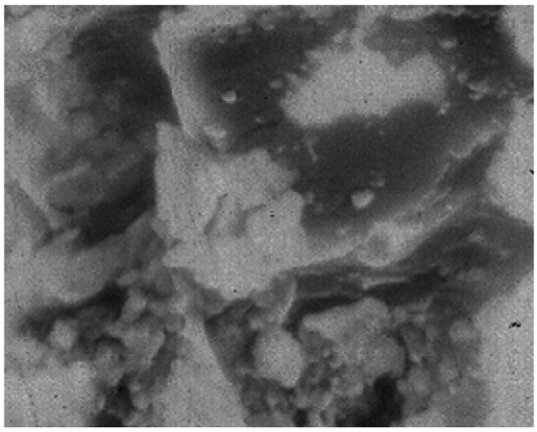

Fig. 7. SEM images of degraded concrete (6000×) from height of 17 m with indistinct crystals of anhydrite.

SEM observations of samples of degraded concrete showed that degraded concrete had highly porous structure and contained crystals of products of chemical degradation. Numerous crystals of gypsum were visible among the aggregate grains in degraded concrete from height of 123 m (Fig. 6). However, the crystals of anhydrite were found in degraded concrete from lower regions of the stack (Fig. 7).

The results of SEM observation corresponded well with findings obtained by wet chemical analyses, XRD and thermal analysis.

4.2. Results of analyses of concrete core

4.2.1. Results of wet chemical analysis of concrete core

Results of wet chemical analysis of the samples of cementitious material that were prepared from the concrete core drilled from the stack shell in height of 15 m above the ground are given in Table 6. The amount of sand and aggregates included in the samples was subtracted from the results.

The chemical composition of the cementitious material of almost all the samples, with the exception of sample 2/4-A, varied in a very narrow range. The content of the sulfates (SO_3) and molar SO_3/CaO ratio was low and almost identical in all the samples from the deeper zones of the concrete (Table 6). To the contrary, the sample 2/4-A from the inside surface zone of the concrete core contained an extremely high content of bound

Table 6
Chemical composition of cementitious material in samples cut from concrete core (wet analysis)

Component	Composition of analyzed samples (%)					
	2/4-A	2/4-B	2/4-C	2/3	2/2	2/1-A
SiO_2 soluble	Missing	15.08	16.14	19.36	18.28	16.27
SO_3	30.62	2.05	2.18	2.01	2.11	2.34
CaO	20.01	41.39	41.03	39.58	42.20	36.57
MgO	1.75	2.56	4.87	5.41	4.16	2.86
R_2O_3	11.01	7.86	8.96	7.51	6.26	10.55
Loss on ignition	22.17	35.28	30.09	28.71	27.76	30.35
SO_3/CaO (molar ratio)	1.072	0.035	0.037	0.036	0.035	0.045

Table 7
pH-values of water suspensions and coloring of concrete by phenolphthalein spraying

	Analyzed sample					
	2/4-A	2/4-B	2/4-C	2/3	2/2	2/1-A
pH	6.8	9.7	12.4	12.3	12.5	12.4
Phenolphthalein coloration	Colorless up → to 20 mm		Purple			Colorless up to 16 mm ←

SO_3, and the molar SO_3/CaO ratio in it was 1.072. It indicates that conversion of calcium compounds and probably also some aluminum and iron compounds to sulfates occurred. The polluted external atmosphere caused a slight increase in the SO_3/CaO ratio also in sample 2/1-A.

4.2.2. Results of water suspension and the phenolphthalein test

The pH-values of the water suspensions from the samples representing the internal regions in the concrete core were ranging from pH 12.3 to 12.5 (Table 7). To the contrary, the pH-values of the water suspensions from samples 2/4-B and 2/4-A that represented the surface zones of drilled concrete were lower. The lowest pH-value of about pH 6.8 was found in water suspension from the surface crust (2/4-A).

The spraying phenolphthalein on the fracture surfaces of the concrete core revealed two colorless zones that were located on both sides of the drilled concrete cylinder (Table 7). The first zone, adjacent to the internal side of the stack shell was about 20 mm thick; the second, adjacent to the external side of the stack was about16 mm thick. The apparent discrepancy between the pH values of the water suspensions and the coloring of the surfaces by phenolphthalein in samples 2/4-B and 2/1-A is caused by different thickness of analyzed zones. Pulverized samples 2/4-B and 2/1-A represent average composition of border zones in the concrete core and they also include uncarbonated parts of concrete.

Table 8
Chemical composition of the binding material on the cross sectional surface of the concrete core measured by EDS

Chemical composition (%)	Depth below the surface of the concrete core (facing inside the stack)					
	100 μm	200 μm	400 μm	800 μm[a]	4000 μm[a]	5000 μm
	Upper yellow zone				Grey zone underneath	
SO_3	51.66	34.90	56.89	21.01	2.95	3.00
CaO	36.18	27.92	39.94	36.73	35.64	56.39
MgO	Traces	Traces	Traces	0.27	0.46	1.78
SiO_2	11.36	27.39	2.54	34.23	48.21	30.57
Al_2O_3	0.08	3.93	0.06	3.81	10.06	4.50
Fe_2O_3	–	2.96	–	2.22	1.37	1.91
K_2O	0.73	2.39	0.57	1.36	1.09	1.34
TiO_2	–	0.52	–	0.39	0.24	0.51
SO_3/CaO (molar ratio)	1.000	0.876	0.997	0.401	0.058	0.037

Chemical composition is expressed as a percentage by the mass of common oxides.
[a] Measured on an unpolished surface.

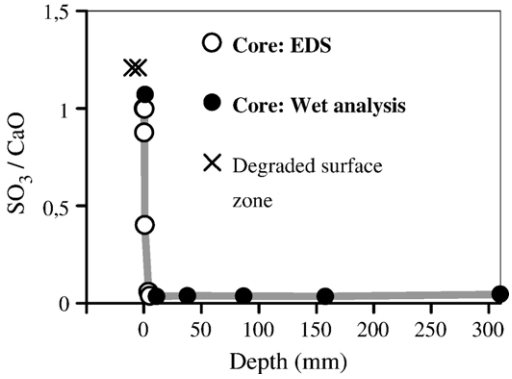

Fig. 8. Molar SO_3/CaO ratio in the cementitious material determined by EDS and wet chemical analyses in various depth of concrete core.

4.2.3. Results of EDS microanalysis of the cementitious material in the concrete core

The chemical composition of the cementitious material in the upper, yellow-colored zone of concrete core (zone 2/4-A in Figs. 2 and 3), and in the gray zone underneath was determined by EDS microanalysis. The results in Table 8 show that the dominant elements in all the analyzed samples are sulfur, calcium and silicon. The sum of SO_3, CaO and SiO_2 ranged from 82% to 88%. Other elements found in much smaller quantity in the samples were iron, aluminum, potassium and titanium.

The analyses confirmed the presence of an extremely high content of sulfur (SO_3) in the upper, yellow-colored zone in the concrete (Table 8, Fig. 8). The molar ratios of SO_3/CaO in this zone were equal or near 1. Also these results indicate that most, if not all, of the calcium compounds from the hardened cement were converted in this zone to sulfur-bearing calcium compounds, which are probably some form of $CaSO_4$. The molar ratios of SO_3/CaO in the gray zone located underneath the yellow crust were about 20 times lower. The results obtained by chemical microanalysis (EDS) and wet chemical analyses are consistent with each other (Fig. 8). They confirm that the sulfur compounds are localized only in the thin upper zone. The relatively higher values in the SiO_2 content in the samples analyzed by EDS are probably due to the small proportion of aggregate particles.

4.2.4. Results of XRD analyses of samples from the concrete core

Crystalline mineral phases composing the samples from the concrete core were identified by XRD analysis (Table 9).

Table 9
Minerals identified by XRD analysis in samples from the concrete core

Sample	Minerals identified	
	Major	Minor and/or traces
2/4-A	Gypsum, quartz	Calcite, feldspars, chlorites
2/4-B	Calcite, quartz	Feldspars, chlorites
2/4-C	Portlandite, calcite, quartz	Feldspars
2/3	Portlandite, calcite, quartz	Feldspars, chlorites
2/2	Portlandite, calcite, quartz	Chlorites
2/1-A	Portlandite, calcite, quartz	Feldspars, chlorites

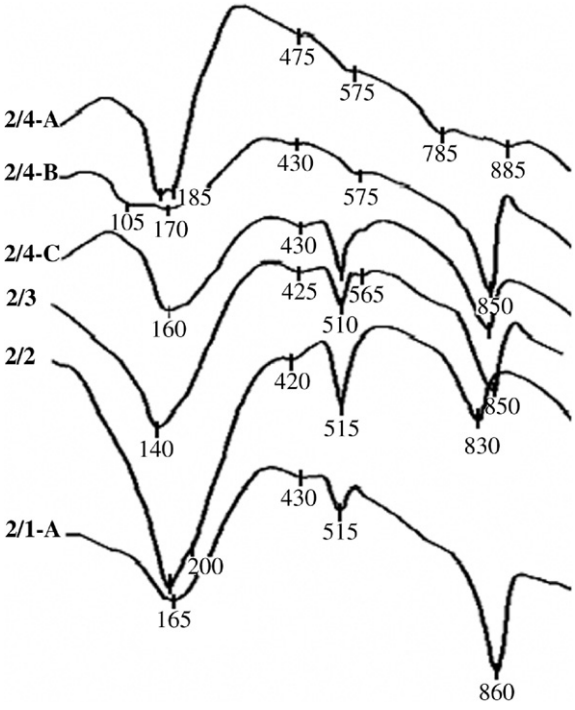

Fig. 9. DTA patterns of cementitious material in samples of the concrete core.

Quartz, feldspars, chlorites, and calcite are minerals that are usually included in natural river-dredged aggregate in the region. Portlandite is a typical product of cement hydration. Calcite and gypsum are products of carbonation and sulfation of the cement stone. However, the calcite from aggregate could not be distinguished by XRD from the calcite, which developed as product of concrete carbonation. Evaluation of aggregate grains from concrete leads to conclusion that most of the $CaCO_3$ in concrete was formed by carbonation of the cementitious material in concrete during operation of the stack.

Gypsum occurred only in the thin crust (zone 2/4-A in Fig. 2) on the internal surface of concrete core. The portlandite was totally absent in zones 2/4-A and 2/4-B. However, it was identified in all the other zones across the stack wall, including the outer external zone 2/1-A. We have to note here again that zone 2/1-A was slightly thicker than the carbonated zone determined by the spraying phenolphthalein.

4.2.5. Results of thermal analyses of samples from concrete core

The results obtained by the differential thermal analyses (Fig. 9) unambiguously proved the presence of gypsum in sample 2/4-A. Calcite and quartz were found in all the samples. Calcium hydroxide was found in samples 2/1-A, 2/2, 2/3 and 2/4-C. Gypsum was identified by its double endothermic effect with peaks at 180 °C and 220 °C on the DTA patterns. The calcite was characterized by one or more endothermic effects appearing in the temperature range from 800 to 1000 °C, quartz by its characteristic endothermic peak at about 570 °C, and calcium hydroxide by an endothermic peak at about 510 °C.

4.3. Results of strengths tests

Results of rebound hammer testing of solid concrete beneath the degraded zone on the internal side of the stack are in Table 10. Table 10 shows that the compressive strength values varied in a very narrow range from 61 to 70.5 MPa along the height of the stack. These assessed compressive strength values were significantly higher than was the designed compressive strength class of the concrete (which corresponded to compressive strength class between C 25/30 and C 30/37 according European standard EN 206-1). The results obtained are satisfactory even if we consider that the compressive strength values obtained by the non-destructive testing method can be more than 20% higher than those determined by destructive testing.

Tensile pull-off strengths of the surface zones of concrete ranged from 1.42 to 3.14 MPa (Table 10). These values were considered satisfactory for the proposed repair works.

5. Summary

Short summary of some relevant results is given in Table 11.

6. Conclusions

Humid flue gases acting at elevated temperatures damaged internal surface of the concrete shell of the coal-fuelled power plant stack. Aggressive acid compounds that include SO_2, SO_3, aerosol/vapor mixture of H_2SO_4 and eventually also nitrogen oxides are mainly responsible for chemical degradation of concrete. Wetting of the surface of concrete by an acid condensate supposedly enhanced aggressiveness of the environment in the stack.

Crumbling zone of degraded concrete covered the surface of concrete shell along the entire inside periphery of the stack. Its thickness varied from 10 to 40 mm, depending on the height along the stack. Analysis of the degraded concrete gives rise to the following conclusions:

1. Attack by acid compounds contained in the flue gases caused total decomposition of the cementitious material in the surface zone of concrete and also partially affected the composition of some minerals in the aggregate. SEM observations showed highly porous structure of degraded concrete.
2. All analyzed samples from the degraded zone contained an extremely high content of sulfates, corresponding to SO_3/CaO molar ratios in the range from 1.01 to 1.21. XRD and thermal

Table 10
Compressive strengths of concrete and tensile strengths of surface zones on internal side of the stack

High (m)	Compressive strength (MPa)	Tensile strength (MPa)
146	62.1	1.52
122	61.0	1.64
97	70.5	2.06
67	67.5	1.65
42	66.8	1.42
16	66.6	3.14

Table 11
Characteristic properties of concrete across the cross-section of the stack shell in height 15 m above the ground

Orientation	← Internal surface							External surface →
	Degraded zone	| Drilled concrete core						
Character Thickness	Sulfated 10 mm	| Sulfated | → 2 mm	Carbonated → 18 mm	Unaffected → 274 mm				Carbonated 16 mm ← |
Sample	K-01-8	2/4A	2/4B	2/4C	2/3	2/2	2/1A	
pH	2.2	6.8	9.7	12.4	12.3	12.5	12.4	
SO_3/CaO	1.21	1.072	0.04	0.04	0.04	0.04	0.05	
Relevant Ca-phases	A (G)	G (C)	P C	P C	P C	P C	P C	

Phases: A — anhydrite, G — gypsum, C — calcite, P — portlandite.

analyses identified mainly gypsum or anhydrite besides quartz and other phases in the samples from this zone. The results show that calcium carbonate and probably all compounds of the cement stone were decomposed and converted into sulfates. The acidic character of water suspensions from these samples, ranging in pH from 2.2 to 6.8, indicated that also some amount of free acid was adsorbed in the degraded material.

3. Chemical and mineralogical composition of the degraded concrete changed along the height in the stack, indicating on its dependence on temperature–humidity conditions in the stack. Conditions in the upper sections of the stack were favorable for formation of gypsum. However, in the lower sections, where the flue gases had higher temperature and lower relative humidity and where also sulfuric acid condensate with higher concentration was assumed the anhydrite formed prevailingly. Degraded concrete from the lower sections also had higher SO_3/CaO molar ratios and formed more acidic water suspensions.

Analyses of the concrete specimen drilled from the stack shell 15 m above ground further indicated the following:

4. Yellowish crust that was composed mostly of gypsum thick about 2–4 mm covered the solid concrete underneath the crumbling surface zone. The SO_3/CaO ratio in the crust zone was equal to or near one. The concrete in this zone entirely lost its alkalinity; giving a pH value of about 7 for its water suspension.
5. A zone of significantly carbonated concrete was located below the sulfated zone. The phenolphthalein spraying showed that the alkalinity of concrete in a zone of about 20 mm thick was lower than pH 9. The thermal and XRD analyses proved that there was almost no calcium hydroxide left in the cementitious material in this zone.
6. These results confirmed the previously reported findings about the combined process of carbonation and sulfation of concrete in an environment containing both sulfur oxides and carbon dioxide. It can be supposed that sulfur oxides and eventually the sulfuric acid diffuse through the wet sulfated layer to the reaction zone underneath, where they react with the cementitious material of carbonated concrete. Calcium carbonate and compounds of cement hydration decompose in the reaction zone and convert to gypsum. Carbon dioxide from the flue gases together with that released from the calcium carbonate diffuses further into the concrete, pushing the carbonated zone deeper. Processes of sulfation and carbonation develop thus simultaneously and their reaction zones move deeper as two parallel fronts.
7. Deeper lying zones of concrete were not affected by carbonation and sulfation and did not show any significant signs of quality decline. The qualitative and quantitative composition of the concrete in these zones did not show any significant differences across the entire thickness of the stack shell.
8. The external side of the concrete shell was also carbonated by the carbon dioxide from the external environment.
9. Finally, it can be concluded that deterioration of the concrete of the stack shell showed signs typical for acidic attack, where relative thin interface zone of gypsum separates the surface zone of totally degraded concrete from the internal zones showing any significant signs of concrete degradation. Results of compressive strength testing of the concrete underneath the degraded cone confirmed this conclusion.

References

[1] D. Damidot, F.P. Glasser, Thermodynamic investigation of the CaO–Al_2O_3–$CaSO_4$–H_2O system at 50 °C and 85 °C, Cem. Concr. Res. 22 (6) (1992) 1179–1191.
[2] A. Gabrišová, J. Havlica, S. Sahu, Stability of calcium sulphoaluminate-hydrates in water solutions with various pH values, Cem. Concr. Res. 21 (6) (1991) 1023–1027.
[3] S.C.B. Myneni, S.J. Traina, T.J. Logan, Ettringite solubility and geochemistry of the $Ca(OH)_2$–$Al_2(SO_4)_3$–H_2O system at 1 atm pressure and 298 K, Chem. Geol. 148 (1–2) (1998) 1–19.
[4] T. Grounds, H.G. Midgley, D.V. Novell, Carbonation of ettringite by atmospheric carbon dioxide, Thermochim. Acta 135 (1988) 347–352.
[5] C. Shi, J.A. Stegemann, Acid corrosion resistance of different cementing materials, Cem. Concr. Res. 30 (2000) 803–808.
[6] E. Scholl, D. Knöfel, On the effect of SO_2 and CO_2 on concrete paste, Cem. Concr. Res. 21 (1) (1991) 27–136.
[7] T. Nishikawa, K. Suzuki, S. Ito, Decomposition of synthesized ettringite by carbonation, Cem. Concr. Res. 22 (1) (1992) 6–14.
[8] A.K. Suryavanshi, R.N. Swamy, Stability of Friedel's salt in carbonated concrete structural elements, Cem. Concr. Res. 26 (5) (1996) 729–741.
[9] V. Fassina, Environmental pollution in relation to stone decay, in: J. Rosvall, S. Aleby (Eds.), Air Pollution and Conservation: Safeguarding our Architectural Heritage, Elsevier, 1998, pp. 133–174.
[10] R. Engelfried, A. Tölle, Effect of moisture and sulphur dioxide content of the air upon the carbonation of concrete, Betonw. Fertigteil–Tech. 11 (1985) 722–729.

[11] D. Knöfel, K.G. Böttger, On the behaviour of cement-bound building materials in an SO_2-enriched atmosphere, Betonw. Fertigteil–Tech. 2 (1985) 107–114.
[12] E. Scholl, D. Knöfel, On the effect of SO_2 and CO_2 on concrete paste, Cem. Concr. Res. 2 (1991) 121–136.
[13] M. Matoušek, R. Drochytka, Atmosférická koroze betonů, IKAS, ČKAIT, Prague, 1998.
[14] N.J. Stevens, Dry SO_2 scrubbing pilot test results, Proceedings of Flue Gas Desulfurization, PB81-243164, 1981, pp. 777–800.
[15] X. Ma, T. Kaneko, T. Tashimo, T. Yoshida, K. Kato, Use of limestone for SO_2 removal from flue gas in the semidry FGD process with a powder-particle spouted bed, Chem. Eng. Sci. 55 (2000) 4643–4652.
[16] A. Garea, J.L. Herrera, J.A. Marques, A. Irabien, Kinetics of dry gas desulfurization at low temperatures using $Ca(OH)_2$: competitive reactions of sulfation and carbonation, Chem. Eng. Sci. 56 (2001) 1387–1393.
[17] X. Ma, T. Kaneko, G. Xu, K. Kato, Influence of gas components on removal of SO_2 from flue gas in the semidry FGD process with a powder-particle spouted bed, Fuel 80 (2001) 673–680.
[18] C.S. Ho, S.M. Shih, Factors influencing the reaction of $Ca(OH)_2$ with SO_2, J. Chin. Inst. Chem. Eng. 24 (1993) 187–195.
[19] J. Klingspor, H.T. Karlsson, I. Bjerle, A kinetic study of the dry SO_2–limestone reaction at low temperature, Chem. Eng. Commun. 22 (1983) 81–103.
[20] B.W. Harris, Conversion of sulfur dioxide to sulfur trioxide in gas turbine exhaust, J. Eng. Gas Turbine Power 112 (1990) 585–589.
[21] R. Hardman, R. Stacy, E. Dismukes, Estimating sulfuric acid aerosol emissions from coal-fired power plants, DOE-FETC Conference on Formation, Distribution, Impact, and Fate of Sulfur Trioxide in Utility Flue Gas Streams, Pittsburgh, PA, March 1998.
[22] V. Číhal, Z. Krhutová, M. Opa, K problémům koroze pod rosným bodem, Kovové materiály v protikorozní ochranì. Konference AKI 98, Beskydy, 1998, (Czech Republic).
[23] F.H. Verhoff, J.T. Banchero, Predicting dew points of flue gases, Chem. Eng. Prog. (1974) (cited in Harris [20]).
[24] K. Malaník, M. Kursová, Korozní podmínky ve výměnících využívajících kondenzační teplo spalin, Konference AKI ′99, Rožnov pod Radhoštěm, 1999, Czech Republic.
[25] S. Martínez-Ramírez, F. Puertas, M.T. Blanco-Varela, G.E. Thomson, Studies on degradation of lime mortars in atmospheric simulation chambers, Cem. Concr. Res. 27 (5) (1977) 777–784.
[26] STN 72 0100 (Slovak standard), Basic analysis of silicates. Common regulations.
[27] EN 196-2 (European standard), Methods of testing cement — Part 2: Chemical analysis of cement.
[28] J. Temuujin, Ts. Jadambaa, K.J.D. Mackenzie, P. Angerer, F. Porte, F. Riley, Thermal formation of corundum from aluminium hydroxides prepared from various aluminium salts, Bull. Mater. Sci. 23 (4) (2000) 301–304.